Eur. J. Biochem. *190*, 113–122 (1990)

Conformational studies on the N-linked carbohydrate chain of bromelain

Jan B. BOUWSTRA, Ellen C. SPOELSTRA, Pieter DE WAARD, Bastiaan R. LEEFLANG, Johannis P. KAMERLING and Johannes F. G. VLIEGENTHART

Department of Bio-Organic Chemistry, Utrecht University, The Netherlands

(Received October 4, 1989/January 30, 1990) – EJB 89 1206

^{1}H- and ^{13}C-NMR assignments for the carbohydrate part of the glycopeptide α-D-Man-(1→6)-[β-D-Xyl-(1→2)]-β-D-Man-(1→4)-β-D-GlcNAc-(1→4)-[α-L-Fuc-(1→3)]-β-D-GlcNAc-(1→N)-Asn∼, derived from the proteolytic enzyme bromelain (EC 3.4.22.4), have been obtained using homo- and heteronuclear correlation spectroscopy, two-dimensional homonuclear Hartmann-Hahn and nuclear Overhauser enhancement experiments. A conformational model for the carbohydrate chain, deduced from the NMR data and consistent with hard-sphere exo-anomeric calculations shows that the rotamer population about the C-5–C-6 bond of β-Man is restricted to the $P_{\omega=180}$ rotamer, mainly.

Xylose-containing N-linked carbohydrate chains have been found as integral parts of plant [1–12] and animal glycoproteins [13–15]. One of the classical examples is the carbohydrate chain of the proteolytic enzyme bromelain from pineapple stem, having the following structure [1, 4];

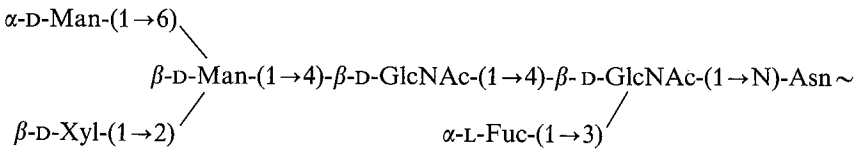

In the framework of our analytical [4, 5, 8, 13–16] and synthetic [17] studies on this type of chains, ^{1}H- and ^{13}C-NMR assignments together with conformational data are reported here for the carbohydrate part of a glycopeptide derived from bromelain. To this end homonuclear Hartmann-Hahn (HOHAHA), double-quantum-filtered ^{1}H-^{1}H correlation spectroscopy (DQF ^{1}H-^{1}H COSY), ^{1}H-^{13}C heterocorrelation spectroscopy (^{1}H-^{13}C COSY) and ^{1}H-^{1}H nuclear Overhauser enhancement (NOE) spectroscopy (^{1}H-^{1}H NOESY), used for build-up rates of the nuclear Overhauser enhancement, have been applied in combination with hard-sphere exo-anomeric effect (HSEA) calculations.

EXPERIMENTAL PROCEDURES

Isolation of bromelain glycopeptide 1

Bromelain preparations (Sigma; approximately 50% protein) were purified to homogeneity using Sephadex G-100 gel filtration and SE- or SP-Sephadex C-50 cation-exchange chromatography [18]. Denatured bromelain (750 mg) was subjected to exhaustive pronase digestion [4] and the mixture of glycopeptides obtained was fractionated on Bio-Gel P-6 (200–400 mesh) [4]. The main glycopeptide fraction was further separated by medium-pressure anion-exchange chromatography on Mono Q with a linear gradient of 0–150 mM NaCl in 5 ml water [19]. Glycopeptide *1*, eluting at 80 mM NaCl, was collected and desalted on Bio-Gel P-2 (200–400 mesh). Sugar analysis [20] revealed the presence of GlcNAc, Fuc, Man and Xyl in the molar ratio of 2.0:1.0:2.0:1.0. Amino acid analysis [21] (Asp:Glu:Ser = 1.0:1.1:1.3) was in agreement with the reported peptide sequence Asn-Glu-Ser-Ser [22].

NMR methods

NMR spectra of an 8 mM glycopeptide solution in ^2H_2O were recorded at 27 °C. Prior to NMR spectroscopy the sample was repeatedly exchanged in 99.75% ^2H_2O with intermediate lyophilisation, finally using 99.96% ^2H_2O (Aldrich). ^{1}H-NMR measurements were carried out on Bruker AM-500 and HX-360 spectrometers (Department of NMR Spectroscopy, Utrecht University) at 500 and 360 MHz, respectively. Resolution enhancement of the spectra was achieved by Lorentzian-to-Gaussian transformation. Chemical shifts (δ) are expressed in ppm downfield from internal sodium 4,4-dimethyl-4-silapentane-1-sulphonate, but were actually measured by reference to internal acetone (δ 2.225 ppm). DQF ^{1}H-^{1}H COSY [23–25] spectra were measured at 500 MHz in the phase-sensitive mode, using quadrature detection in *F2* and time-proportional phase increments [25], resulting in pure absorption/dispersion line-shapes without phase-twist. HOHAHA spectra [26, 27] were obtained at 500 and at 360 MHz. For the 500-MHz HOHAHA spectrum a field strength of 8.33 kHz (60-μs 180° pulse width) was used and

Correspondence to J. P. Kamerling, Department of Bio-Organic Chemistry, Utrecht University, Transitorium III, P.O. Box 80.075, NL-3508 TB Utrecht, The Netherlands

Abbreviations. Xyl, xylose; Fuc, fucose; 1D, one-dimensional; 2D, two-dimensional; NOESY, nuclear Overhauser enhancement spectroscopy; COSY, correlation spectroscopy; HOHAHA, homonuclear Hartmann-Hahn; DQF, double quantum filtered; MLEV, Malcom Levitt; HSEA, hard-sphere exo-anomeric.

Enzyme. Bromelain (EC 3.4.22.4).

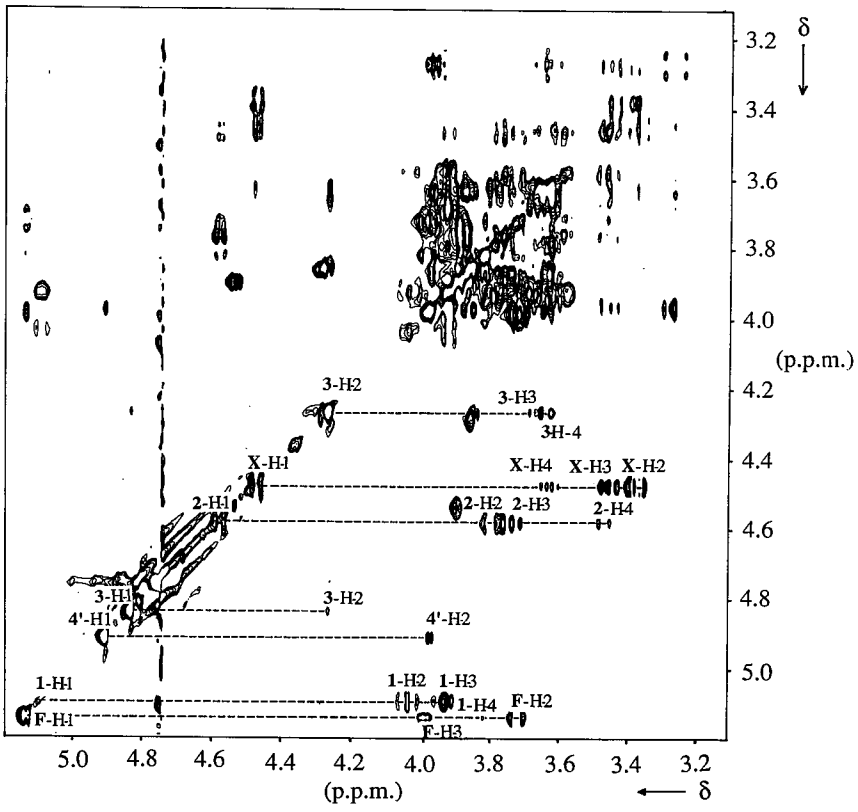

Fig. 1. *360-MHz HOHAHA spectrum of α-Man-(1→6)-[β-Xyl-(1→2)]-β-Man-(1→4)-β-GlcNAc-(1→4)-[α-Fuc-(1→3)]-β-GlcNAc-(1→N)-Asn* ~. The mixing time is 40 ms. Lines are drawn to show scalar coupled networks. **3**-H-2 means H-2 of Man-**3**, **X**-H-2 means H-2 of Xyl and **F**-H-2 means H-2 of Fuc, etc.

the mixing period consisted of 60 Malcom Levitt (MLEV)-17 cycles, resulting in a 120-ms mixing time. For the 360-MHz HOHAHA spectrum a field strength of 12.1 kHz (41.2-μs 180° pulse width) was used and a compensated phase-alternating mixing period of 40 ms was applied. For the NOESY experiments [28] the sample was degassed in the NMR tube by repeated evacuation, and sealed under argon. To determine the initial cross-relaxation rate [29], mixing times of 75, 150, 250 and 350 ms were used. Spectra were measured in the phase-sensitive mode, using quadrature detection in *F2* and time-proportional phase increments [25]. In each 2D ^{1}H-NMR experiment, the spectral width was 3333.33 Hz in both dimensions, and 512 measurements with t_1 values ranging over 0.075 – 76.8 ms were recorded for one experiment. A 512 × 4K data matrix was acquired which was zero-filled and multiplied in both dimensions with a phase-shifted sine-square prior to a phase-sensitive Fourier transformation to obtain a 2K × 4K spectral data matrix.

Natural-abundance proton-decoupled ^{13}C-NMR spectroscopy was carried out at 50.76 MHz on a Bruker WM-200 spectrometer (SON hf-NMR-facility, Department of Biophysical Chemistry, University of Nijmegen) equipped with a 5-mm broad-band probe. The spectral width was 10000 Hz. Chemical shifts (δ) are given in ppm downfield from external Me_4Si, but were actually measured by reference to internal acetone (δ31.55 ppm). ^{1}H-^{13}C COSY was performed with simultaneous suppression of ^{1}H-homonuclear-couplings [30, 31] using the standard Bruker program XHCORRD and a phase cycling of the refocussing pulse [32]. Refocussing delays were adjusted to an average $J_{C\text{-}H}$ coupling constant of 150 Hz. The ^{13}C and ^{1}H 90° pulse widths were determined to be 8 and 12 μs, respectively (cf. [33]). A 64 × 4K data matrix was acquired, which was zero-filled prior to Fourier transformation to obtain a 1K × 8K spectral data matrix. To enhance resolution a non-shifted cosine-squared function for ^{13}C subspectra and a π/3-shifted sine-squared function for ^{1}H subspectra were applied.

Distance constraints

To obtain the initial-rate cross-peak intensity, the NOE cross-peak intensities, measured with different mixing times τ, have to be fitted to the exponential function $I_{\tau,rel} = I_{\tau\text{-max}} - (I_{\tau\text{-max}} - I_{\tau\text{-min}})^* e^{-k\tau}$ ($I_{\tau,rel}$, cross-peak intensity, relative to diagonal cross-peak intensity; $I_{\tau\text{-max}}$, relative cross-peak intensity in spectrum with longest τ; $I_{\tau\text{-min}}$, relative cross-peak intensity in spectrum with shortest τ) by the minimum least-square method, and the initial rate of the NOE build-up is given by k^* ($I_{\tau\text{-max}} - I_{\tau\text{-min}}$). Inter-residue ^{1}H – ^{1}H distances are calculated by relating their initial-rate NOE cross-peak intensities to the initial-rate cross-peak intensities of intraresidue ^{1}H – ^{1}H pairs at known distances from each other (0.22 – 0.26 nm [34]) by the equation $r_{ij} = r_0(a_0/a_{ij})^{1/6}$ (r_{ij}, distance to be determined; r_0, known distance; a_{ij}, initial-rate cross-peak intensity of a pair of protons at an unknown distance; a_0, initial-rate cross-peak intensity of a pair of protons at a known distance) [29].

Energy calculations and molecular modelling

The HSEA program [35 – 38], taking into account non-bonded interactions as expressed by the Kitaigorodsky algorithm, together with a term for the exo-anomeric effect, was used to estimate minimum energy conformations together with the rotational freedom of every glycosidic linkage. In the

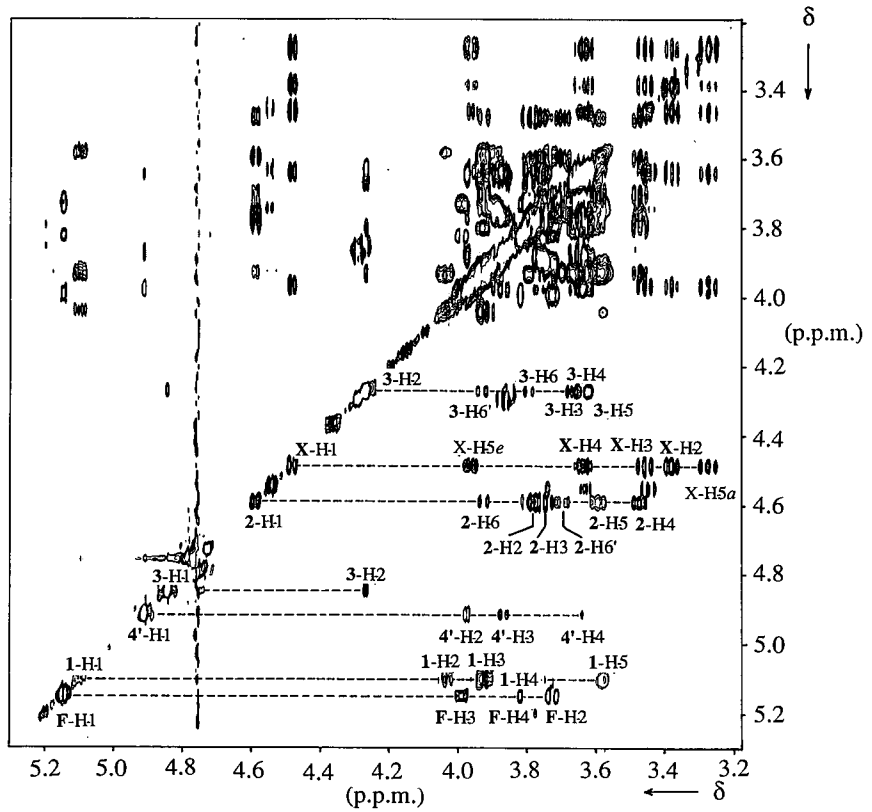

Fig. 2. *500-MHz HOHAHA spectrum of α-Man-(1→6)-[β-Xyl-(1→2)]-β-Man-(1→4)-β-GlcNAc-(1→4)-[α-Fuc-(1→3)]-β-GlcNAc-(1→N)-Asn* ~. The mixing time is 120 ms. Lines are drawn to show scalar coupled networks. **3**-H-2 means: H-2 of Man-**3**, etc. as in Fig. 1

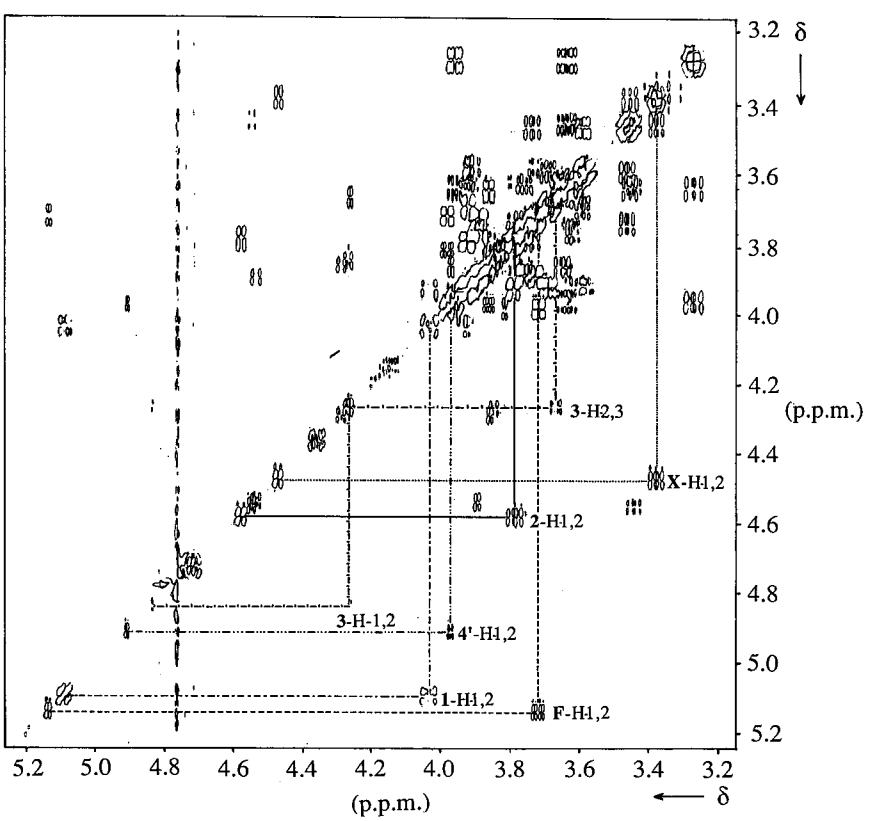

Fig. 3. *500-MHz ^1H-^1H COSY spectrum of α-Man-(1→6)-[β-Xyl-(1→2)]-β-Man-(1→4)-β-GlcNAc-(1→4)-[α-Fuc-(1→3)]-β-GlcNAc-(1→N)-Asn* ~. Lines are drawn to show some correlations present. **3**-H-1,2 means: cross-peak between H-1 and H-2 of Man-**3**, etc.

Table 1. *^{1}H-chemical shifts of the constituent monosaccharides of glycopeptide* 1
Chemical shifts (δ) are expressed in ppm downfield from internal sodium 4,4-dimethyl-4-silapentane-1-sulfonate in ^2H_2O at 27°C acquired at 500 and 360 MHz, but were actually measured by reference to internal acetone (δ 2.225 ppm). For the numbering of the monosaccharides, see the formula

Atom	Chemical shift in residue					
	GlcNAc-**1**	GlcNAc-**2**	Man-**3**	Man-**4′**	Xyl	Fuc
	ppm					
H-1	5.121	4.579	4.839	4.913	4.470	5.136
H-2	4.033	3.786	4.262	3.972	3.376	3.721
H-3	3.924	3.735	3.665	3.863	3.452	3.981
H-4	3.920	3.458	3.615	3.640	3.637	3.814
H-5	3.575	3.590	3.618	3.620	3.270(H-5*a*) 3.961(H-5*e*)	4.722
H-6	3.892	3.920	3.785	3.770	–	–
H-6′	3.723	3.691	3.920	3.887	–	–
NAc	1.994	2.066	–	–	–	–
CH_3	–	–	–	–	–	1.285

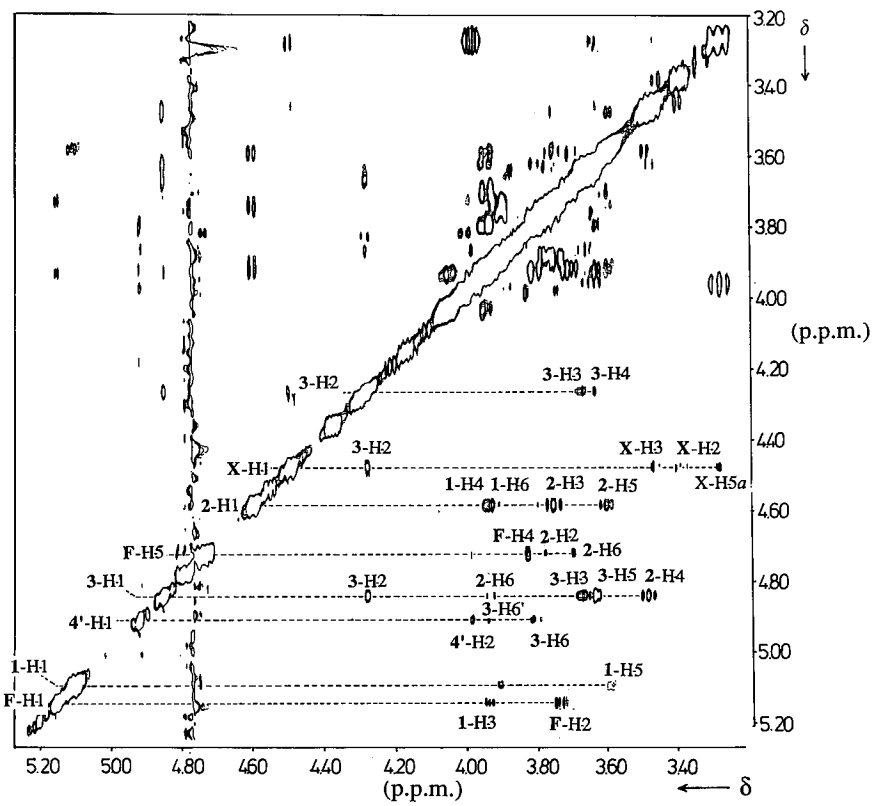

Fig. 4. *500-MHz ^1H-^1H NOESY spectrum of α-Man-(1→6)-[β-Xyl-(1→2)]-β-Man-(1→4)-β-GlcNAc-(1→4)-[α-Fuc-(1→3)]-β-GlcNAc-(1→N)-Asn* ~. The mixing time is 250 ms. **3**-H-2 means: H-2 of Man-**3**, etc.

φ/ψ domain iso-energy contour levels were calculated with steps of 2.1 kJ/mol (0.5 kcal/mol). The torsional angle φ is defined as (H-1′,C-1′,O,C-x) with x = 2, 3, 4 or 6; the torsional angle ψ as (C-1′,O,C-x,H-x) with x = 2, 3 or 4, and as (C-1′,O,C-6,C-5) for (1→6)-linkages; the bond angle τ (C-1′, O,C-x) is set at 117°.

The rotamer population about the C-5–C-6 bond of β-Man is calculated from the spin-spin couplings $J_{5,6}$ and $J_{5,6'}$ [39]. The torsional angle ω is defined as (O-6,C-6,C-5,H-5).

Molecular modelling has been carried out on an Evans & Sutherland PS 300 graphic display station and the geometry calculations were performed on a local VAX cluster by use of the program PLATON [40].

RESULTS

^{1}H-NMR assignments

The HOHAHA (mixing times 40 and 120 ms) and the DQF ^{1}H-^{1}H COSY spectra of glycopeptide *1* are depicted in Figs 1, 2 and 3, respectively. A survey of the ^{1}H-NMR assignments is given in Table 1. To obtain complete assign-

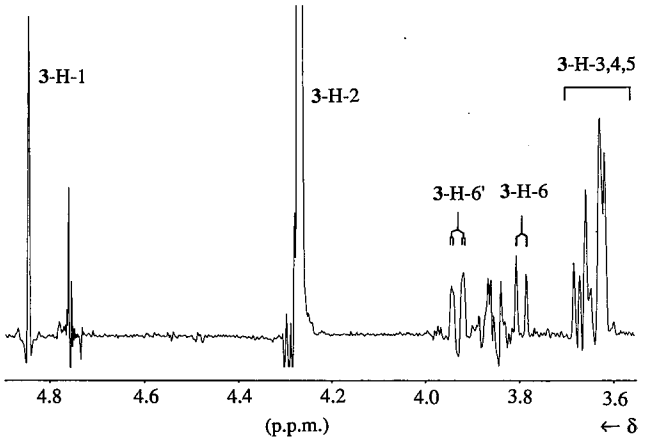

Fig. 5. *Subspectrum at δ 4.262 ppm (Man-3 H-2 track) of the 120-ms HOHAHA spectrum of α-Man-(1→6)-[β-Xyl-(1→2)]-β-Man-(1→4)-β-GlcNAc-(1→4)-[α-Fuc-(1→3)]-β-GlcNAc-(1→N)-Asn ~.* 3-H-6 means: H-6 of Man-3, etc.

ments of the 2D spectra, the earlier identified H-1 signals [4] are used as starting points. For Xyl, the H-1 resonance is observed at δ 4.470 ppm. The 40-ms HOHAHA spectrum shows at the Xyl H-1 track transfer of the magnetisation from H-1 to H-2,3,4. The assignments of the final protons are made on the basis of cross-peaks in the DQF ^{1}H-^{1}H COSY spectrum. In the 120-ms HOHAHA spectrum a further transfer of this magnetisation to H-5*a*,5*e* is realised. The starting point for the assignments of the Man-4′ resonances is the H-1 doublet at δ 4.913 ppm [4]. The 40-ms HOHAHA spectrum shows the H-2 resonance at the Man-4′ H-1 track and the 120-ms HOHAHA spectrum reveals at this track the H-3 and H-4 resonances in addition. The H-3 and H-4 resonances are discriminated on the basis of cross-peaks in the DQF ^{1}H-^{1}H COSY spectrum. The H-2 track (δ 3.972 ppm) in the 120-ms HOHAHA spectrum shows the H-3,4,5,6,6′ resonances, and the H-5, H-6 and H-6′ resonances are assigned on the basis of the characteristic H-6,6′ and H-5,6′ cross-peaks in the DQF ^{1}H-^{1}H COSY spectrum. The Man-3 H-1 resonance is found at δ 4.839 ppm [4]. The 40-ms HOHAHA spectrum shows the H-2 resonance at the Man-3 H-1 track and the H-3,4 resonances at the Man-3 H-2 track (δ 4.262 ppm). H-3 and H-4 are discriminated on the basis of cross-peaks in the DQF ^{1}H-^{1}H COSY spectrum. In the 40-ms HOHAHA spectrum no further magnetisation transfer is observed due to small coupling constants between H-1,2 as well as H-2,3. The 120-ms HOHAHA spectrum shows only the H-2 resonance at the H-1 track, but at the H-2 track the magnetisation is transferred up to and including the H-6,6′ resonances. The overlapping H-4 and H-5 resonances have been assigned by a ^{1}H-^{1}H NOESY experiment (Fig. 4), showing strong H-1,3 and H-1,5 NOE cross-peaks for Man-3. The remaining H-6 and H-6′ cross-peaks have been interpreted on the basis of their coupling pattern in the cross-section at the Man-3 H-2 track (Fig. 5) of the 120-ms HOHAHA spectrum. For GlcNAc-2 the 40-ms HOHAHA spectrum exhibits at the H-1 track (δ 4.579 ppm) H-2,3,4, whereas the 120-ms HOHAHA spectrum shows at this track the complete GlcNAc-2 subspectrum. In conjunction with the observed H-1,2, H-3,4, H-4,5, H-5,6 and H-6,6′ cross-peaks in the DQF ^{1}H-^{1}H COSY spectrum the resonances for GlcNAc-2 could be assigned unequivocally. For GlcNAc-1 the 40-ms HOHAHA spectrum reveals the H-2,3,4 resonances on the H-1 track (δ 5.121 ppm [4]) with the H-3 and H-4 cross-peaks nearly coinciding. A cross-peak between the H-4 resonance of GlcNAc-1 and the H-1 resonance of GlcNAc-2 in the ^{1}H-^{1}H NOESY spectrum shows H-4 to resonate at 3.920 ppm, whereas the H-2,3 cross-peak in the DQF ^{1}H-^{1}H COSY spectrum reveals H-3 to resonate at δ 3.924 ppm. On the H-1 track in the 120-ms HOHAHA spectrum the resonances for H-2,3,4,5 are observed. In addition, connectivities for H-5,6,6′ are found on the H-5 track (δ 3.575 ppm) in the 40-ms HOHAHA spectrum. This spectrum shows at the Fuc H-1 track (δ 5.136 ppm [4]) the H-2,3 resonances, whereas the 120-ms HOHAHA spectrum shows the H-4 resonance at this track in addition. The H-2 and H-3 resonances are distinguished by the H-1,2 cross-peak in the DQF ^{1}H-^{1}H COSY spectrum. The H-5 chemical shift is assigned by the cross-peak between H-5 and CH_3 [4].

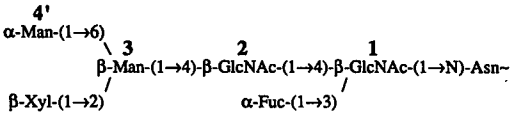

1

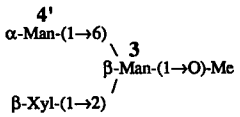

2

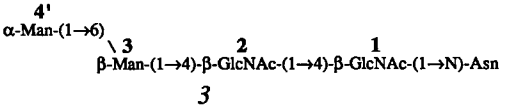

3

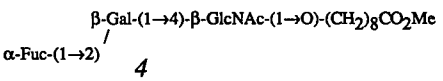

4

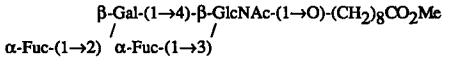

5

^{13}C-NMR assignments

The ^{13}C-NMR data of the carbohydrate part of glycopeptide *1* are summarised in Table 2. Owing to the low amount of material, the assignments of the ^{13}C resonances could not be made on the basis of the ^{1}H-^{13}C COSY spectrum only. For this reason use has been made of the ^{13}C-NMR data of the reference compounds *2*–*5* [16, 41, 42] (Table 2). The ^{13}C resonances of Xyl, Man-4′ and Man-3 have been assigned on the basis of the corresponding data of compound *2*. Comparison of the ^{13}C-NMR data of *1* and *3* shows that the attachment of Xyl at C-2 of Man-3 results in a downfield shift for the resonance of Man-3 C-2 (Δδ +7.34 ppm) and in upfield shifts for the resonances of Man-3 C-1 and C-3 (Δδ −0.53 and −0.92 ppm, respectively). The ^{13}C resonances of GlcNAc-2 in *1* have been established by comparison with the ^{13}C-NMR data of *3*, and the positions of C-4 and C-5 have been proved by ^{1}H-^{13}C COSY. The observed chemical shift differences for GlcNAc-2 C-4 (Δδ +1.12 ppm) and C-5 (Δδ −1.45 ppm) in *1* and *3* may be ascribed to the presence of α-Fuc (1→3)-linked to GlcNAc-1. For Fuc, the ^{13}C resonances in *1* have been obtained by comparison with the data of *5*, whereby the position of the C-2 resonance has been derived

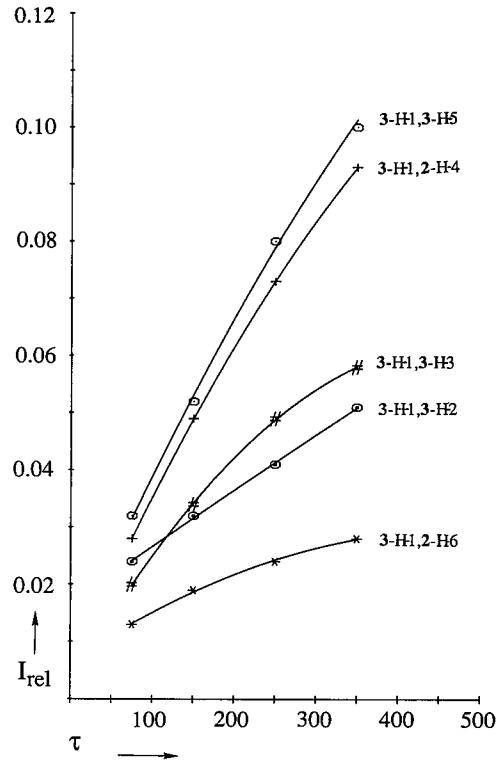

Fig. 6. *Dependence of the relative peak heights* I_{rel} *on the mixing time* τ *of cross-peaks in the* ^1H-^1H *NOESY spectrum of* α-*Man-(1→6)-[*β-*Xyl-(1→2)]-*β-*Man-(1→4)-*β-*GlcNAc-(1→4)-[*α-*Fuc-(1→3)]-*β-*GlcNAc-(1→N)-Asn*∼, *as shown for the magnetization transfer from H-1 of Man-3 to the nearby protons.* These data are measured in a cross-section through the diagonal peak of H-1 of Man-**3**

from ^1H-^{13}C COSY. The chemical shifts of the resonances for C-1, C-2 and C-6 of GlcNAc-**1** are assessed by comparison with the data of *3* and the chemical shifts of the resonances for C-3, C-4 and C-5 are assigned by the ^1H-^{13}C COSY experiment. It is noteworthy that, compared to *3*, the α-(1→3)-fucosylation strongly influences the position of the C-3, C-4 and C-5 resonances ($\Delta\delta$ + 3.98 ppm, −3.86 ppm and − 1.94 ppm, respectively). Comparable shifts for C-3 and C-4 were found in the step from *4* to *5*.

Conformational analysis

In Table 3 the initial-rate cross-relaxation data, calculated from the ^1H-^1H NOESY spectra with mixing times of 75, 150, 250 (Fig. 4) and 350 ms, respectively, are presented. As a typical example, in Fig. 6 the I_{rel}/τ curves are shown for the magnetisation transfer from Man-**3** H-1 to the nearby protons. The use of NOE build-up rates permits an accurate interpretation of NOE data in terms of ^1H-^1H distances, because spin diffusion artefacts can be excluded to a large extent [29]. Owing to the signal/noise ratio in the ^1H-^1H NOESY spectra, only the NOE build-up ranges for protons within 0.30 nm from each other are taken into account. From the absence of an NOE cross-peak between two protons it is concluded that these are more than 0.30 nm from each other. In Table 3 also the calculated ^1H-^1H distances for inter-residue ^1H-^1H pairs are presented, together with intraresidue ^1H-^1H distances [34] as references. To determine the maximum inaccuracy in the calculation of the initial-rate cross-relaxation data, the reported intraresidue distances [34] were compared with those calculated from the initial-rate cross-peak intensities. The maximum deviation was found to be 10%, corresponding to an inaccuracy of 2% for the calculated ^1H-^1H distances.

HSEA calculations have been used to establish the iso-energy contours (Fig. 7) for the glycosidic linkages and to estimate ^1H-^1H distances as a function of the torsional angles φ and ψ. In the following, each glycosidic linkage will be discussed separately.

β-Xyl-(1→2)-Man-linkage. The interglycosidic NOE effect between H-1 of Xyl and H-2 of Man-**3** indicates a distance of 0.23 nm between these protons (Table 3). All φ/ψ combinations allowed by this distance constraint are marked in the iso-energy contour map in Fig. 7a. The HSEA calculations in combination with the distance constraint leads to φ/ψ = 50/0 for the conformation about the β-Xyl-(1→2)-Man-linkage (Table 4). It should be noted that the conformation of the linkage can not be derived from the ^1H-NMR data alone, because one interglycosidic distance constraint points only to a range of φ/ψ values. The iso-energy contours are not changed substantially by extending the disaccharide with GlcNAc-**2** (data not shown).

α-Man-(1→6)-Man-linkage. To determine the orientation of α-Man (1→6)-linked to β-Man the rotamer population about the C-5−C-6 bond is calculated [39] from the vicinal coupling constants $J_{5,6}$ (≈1 Hz) and $J_{5,6'}$ (2.1 Hz) as measured from the H-6 and H-6′ signals in the subspectrum at δ 4.262 ppm (Man-**3** H-2 track) in the 120-ms HOHAHA spectrum (Fig. 5). These values reflect a rotamer population dominated by the $P_{\omega=180}$ rotamer (>98%). Analysis of cross-relaxation rates between H-1 of Man-**3** and H-6,6′ of Man-**4**′ shows the H-1−H-6 and the H-1−H-6′ distances to be 0.24 and 0.30 nm, respectively. In the energy profile for the $P_{\omega=180}$ rotamer (Fig. 7b) the φ/ψ areas, deduced from the distance constraints, are marked. The cross-section of both distance constraints at φ/ψ = −40/170 (Table 4) defines the time-averaged conformation about the (1→6)-linkage.

β-Man-(1→4)-GlcNAc-linkage. NOE effects between H-1 of Man-**3** and H-4,6 of GlcNAc-**2** show the H-1−H-4 and H-1−H-6 distances to be 0.24 and 0.29 nm, respectively (Table 3). The φ/ψ areas deduced from these distance constraints are marked in the iso-energy contour map in Fig. 7c, showing that the H-1−H-4 distance constraint limits φ and the H-1−H-6 ψ. The cross-section of both areas at φ/ψ = 60/0 reflects the conformation of the (1→4)-linkage, in accordance with the HSEA calculations.

β-GlcNAc-(1→4)-GlcNAc-linkage. NOE effects between H-1 of GlcNAc-**2** and H-4 of GlcNAc-**1** and between H-1 of GlcNAc-**2** and H-6 of GlcNAc-**1** point to distance constraints of 0.24 and 0.27 nm (Table 3), respectively, and determine the conformation about the (1→4)-linkage to be φ/ψ = 50/10 (Table 4), in agreement with the HSEA calculations (Fig. 7d). A comparison of the φ/ψ maps for the glycosidic linkage of this disaccharide with and without Fuc, α-(1→3)-linked to GlcNAc-**1** (data not shown), shows that the potential energy well is considerably narrowed by Fuc, but not shifted to other φ/ψ regions.

α-Fuc-(1→3)-GlcNAc-linkage. NOE effects between H-3 of Fuc and H-6′ of GlcNAc-**2**, H-5 of Fuc and H-2 of GlcNAc-**2**, and H-1 of Fuc and H-3 of GlcNAc-**1** indicate distances of 0.24, 0.27 and 0.25 nm, respectively. All φ/ψ combinations deduced from these distance constraints are marked in the iso-energy contour map (Fig. 7e). The cross-section determines φ/ψ to be 45/30. HSEA calculations for the α-Fuc-(1→3)-GlcNAc-linkage show that the orientation of α-Fuc is influenced by the attachment of GlcNAc-**2**, yielding φ/ψ = 50/25

Table 2. *^{13}C-chemical shifts of the constituent monosaccharides of glycopeptide* 1 *and the reference structures* 2 *[16],* 3 *[41],* 4 *and* 5 *[42]*
Chemical shifts (δ) are expressed in ppm downfield from external Me_4Si in ^2H_2O at 27°C acquired at 50 MHz, but were actually measured by reference to internal acetone (δ 31.55 ppm). For the numbering of the monosaccharides, see the formula

Residue	Atom	Chemical shift in carbohydrate				
		1	*2*	*3*	*4*	*5*
		ppm				
GlcNAc-**1**	C-1	79.28		79.61	102.35	102.22
	C-2	55.62		55.12	56.71	57.39
	C-3	78.25		74.27[f]	73.58	76.94
	C-4	76.40		80.26	77.72	74.62
	C-5	75.84[a]		77.78	76.58	76.18
	C-6	61.04		61.45	61.59	61.29
	CH_3	23.51[b]		23.63		
GlcNAc-**2**	C-1	102.04		102.83		
	C-2	56.39		56.45		
	C-3	73.66		73.53[f]		
	C-4	82.30		81.18		
	C-5	74.50		75.95		
	C-6	62.21[c]		61.63		
	CH_3	23.52[b]		23.77		
Man-**3**	C-1	101.56	102.66	102.09		
	C-2	79.28	79.56	71.94		
	C-3	73.35	73.41	74.27		
	C-4	68.32	68.47	68.36		
	C-5	75.83[a]	75.77	75.95		
	C-6	67.14	67.03	67.75		
Man-**4′**	C-1	101.11	100.90	101.26		
	C-2	71.12	71.19	71.45		
	C-3	71.74	71.90	71.94		
	C-4	68.03[d]	67.98	68.36		
	C-5	74.01	74.00	74.27		
	C-6	62.50[c]	62.21	62.51		
α-(1→3)-Fuc	C-1	99.64				99.87
	C-2	69.04				69.65
	C-3	70.57[e]				70.53
	C-4	73.07				73.26
	C-5	68.04[d]				68.15
	CH_3	16.84				16.81
Xyl	C-1	105.50	105.48			
	C-2	74.59	74.56			
	C-3	76.67	76.73			
	C-4	70.51[e]	70.52			
	C-5	66.39	66.42			

[a–e] ^{13}C chemical shifts might be interchanged between each of these five pairs of atoms
[f] ^{13}C chemical shifts are interchanged between this pair of atoms, according to [43]

(Fig. 7e) in the presence of GlcNAc-**2** and φ/ψ = 45/15 in the absence of GlcNAc-**2** (data not shown).

DISCUSSION

The assignments of the ^{1}H-NMR spectra for the carbohydrate part of glycopeptide *1* have made possible a conformational analysis of all glycosidic linkages. The linkage conformations are expressed by the parameters φ and ψ with an inaccuracy of $\pm 5°$. Except for the β-Xyl-(1→2)-Man-linkage, all conformations can be deduced from ^{1}H-NOE data only. It was found that the φ/ψ values for the β-GlcNAc-(1→4)-GlcNAc-linkage are identical to those calculated for this linkage in case of a non-fucosylated *N,N′*-diacetylchitobiose unit [44], indicating that the conformation is not substantially influenced by the α-(1→3)-attachment of Fuc. According to the measured coupling constants the rotamer population about the C-5 – C-6 linkage of Man-**3** is dominated by the presence of the $P_{\omega=180}$ rotamer. A comparison of the rotamer populations about the C-5 – C-6-linkage of Man-**3** for a variety of oligosaccharides, obtained by calculation from $J_{5,6}$ and $J_{5,6'}$ values, shows that the rotamer population can vary considerably [45]. For α-Man-(1→6)-[α-Man-(1→3)]-β-Man-(1→4)-β-GlcNAc-(1→4)-β-GlcNAc-ol [45] and for a conventional asialo diantennary alditol [45 – 47] the rotamer population is characterized by the clear presence of both the $P_{\omega=180}$ and $P_{\omega=-60}$ rotamers. The $P_{\omega=180}$ rotamer only has been found for an asialo bisected diantennary alditol [45, 47] and for an oligomannose structure [$(Man)_9(GlcNAc_2)$ol] [47]. For α-Man-(1→6)-[α-Man-(1→3)]-[β-Xyl-(1→2)]-β-Man-(1→4)-β-GlcNAc-(1→4)-[α-Fuc-(1→3)]-β-GlcNAc-(1→N)-Asn the presence of both the $P_{\omega=180}$ and $P_{\omega=-60}$ conformers has

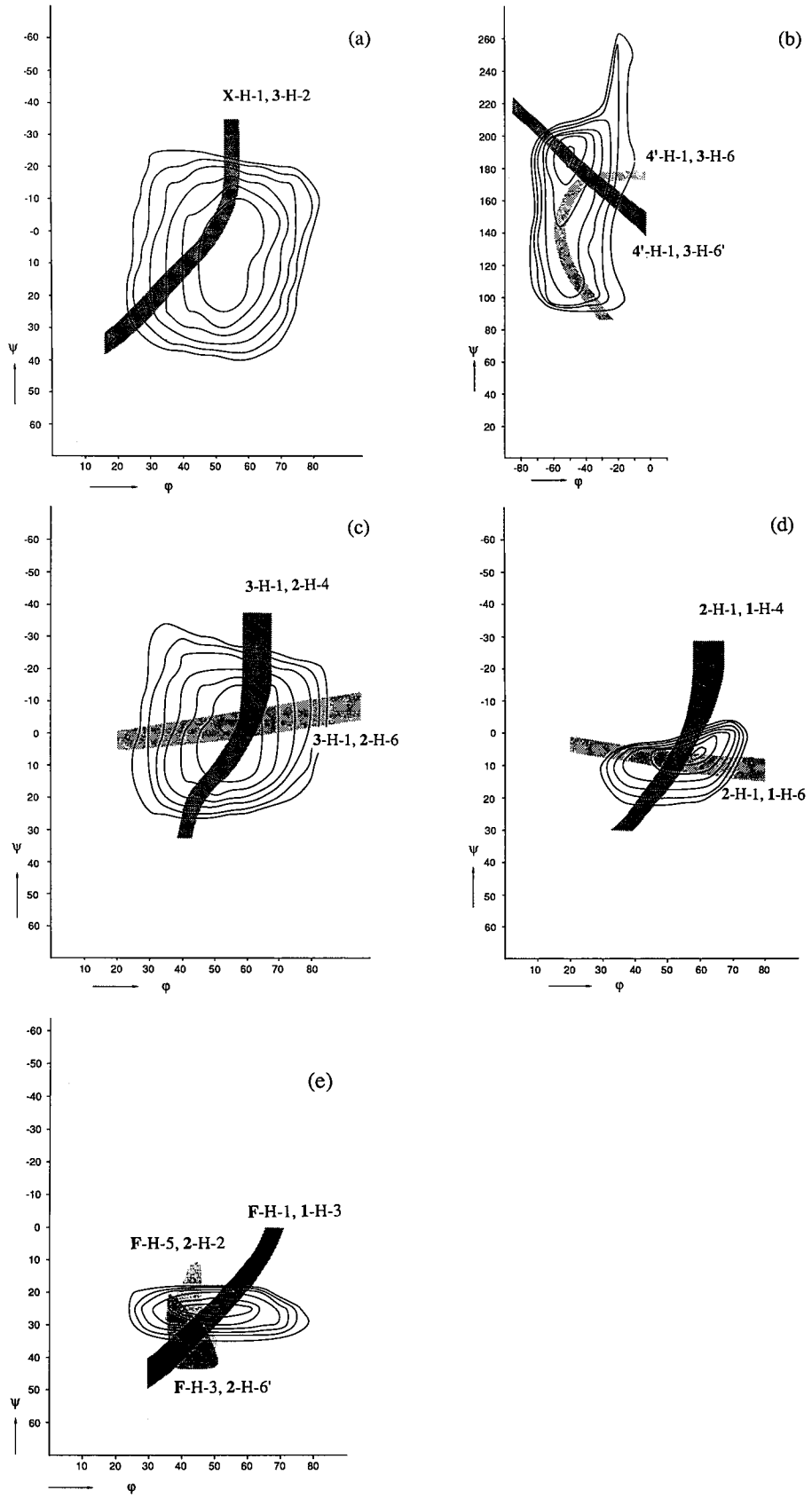

Fig. 7. *The iso-energy contour maps of (a) the β-Xyl-(1→2)-Man linkage, (b) the α-Man-(1→6)-Man linkage for the* $P_{\omega=180}$ *rotamer, (c) the β-Man-(1→4)-GlcNAc linkage, (d) the β-GlcNAc-(1→4)-GlcNAc linkage with α-Fuc (1→3)-linked to GlcNAc-**1**, (e) the α-Fuc-(1→3)-GlcNAc linkage with β-GlcNAc (1→4)-linked to GlcNAc-**1**.* Marked areas with the φ/ψ combinations deduced from the experimentally obtained distance constraints are included. **X**-H-1,**3**-H-2 means: all φ/ψ combinations indicated by the NOE effect between H-1 or Xyl and H-2 of Man-**3**

Table 3. *Initial cross-relaxation rates, reference intraresidue distances and calculated inter-residue distances between protons of constituent monomers of glycopeptide* 1

Intraresidue distances [34]	^1H-^1H connectivity	Intial-rate cross-relaxation	Calculated inter-residue distances
nm			nm
0.26	H-1 Xyl: H-3 Xyl	$1.65 \cdot 10^{-2}$	
0.24	H-1 Xyl: H-5*a* Xyl	$2.80 \cdot 10^{-2}$	
	H-1 Xyl: H-2 Man-**3**	$3.55 \cdot 10^{-2}$	0.23
0.26	H-1 Man-**4**′: H-2 Man-**4**′	$1.55 \cdot 10^{-2}$	
	H-1 Man-**4**′: H-6 Man-**3**	$2.75 \cdot 10^{-2}$	0.24
	H-1 Man-**4**′: H-6′ Man-**3**	$0.70 \cdot 10^{-2}$	0.30
0.26	H-1 Man-**3**: H-2 Man-**3**	$1.60 \cdot 10^{-2}$	
0.25	H-1 Man-**3**: H-3 Man-**3**	$2.40 \cdot 10^{-2}$	
0.24	H-1 Man-**3**: H-5 Man-**3**	$2.95 \cdot 10^{-2}$	
	H-1 Man-**3**: H-4 GlcNAc-**2**	$2.95 \cdot 10^{-2}$	0.24
	H-1 Man-**3**: H-6 GlcNAc-**2**	$1.00 \cdot 10^{-2}$	0.29
0.24	H-1 GlcNAc-3: H-5 GlcNAc-**2**	$3.00 \cdot 10^{-2}$	
	H-1 GlcNAc-**2**: H-4 GlcNAc-**1**	$2.70 \cdot 10^{-2}$	0.24
	H-1 GlcNAc-**2**: H-6 GlcNAc-**1**	$1.40 \cdot 10^{-2}$	0.27
0.25	H-1 Fuc: H-2 Fuc	$2.10 \cdot 10^{-2}$	
	H-1 Fuc: H-3 GlcNAc-**1**	$2.25 \cdot 10^{-2}$	0.25
0.23	H-5 Fuc: H-4 Fuc	$3.00 \cdot 10^{-2}$	
	H-5 Fuc: H-2 GlcNAc-**2**	$1.10 \cdot 10^{-2}$	0.27
	H-3 Fuc: H-6′ GlcNAc-**2**	$2.30 \cdot 10^{-2}$	0.24

Table 4. *Torsional angles (φ,ψ) for the various glycosidic linkages of glycopeptide* 1 *and the rotamer population about the C-5 – C-6 bond of β-D-Man, as determined by ^1H-NMR measurements in combination with HSEA calculations*

Linkage	φ/ψ	$P_{\omega=180}$
		%
β-Xyl-(1→2)-Man	50/0	
α-Man-(1→6)-Man	−40/170	>98
β-Man-(1→4)-GlcNAc	60/0	
β-GlcNAc-(1→4)-GlcNAc	50/10	
α-Fuc-(1→3)-GlcNAc	45/30	

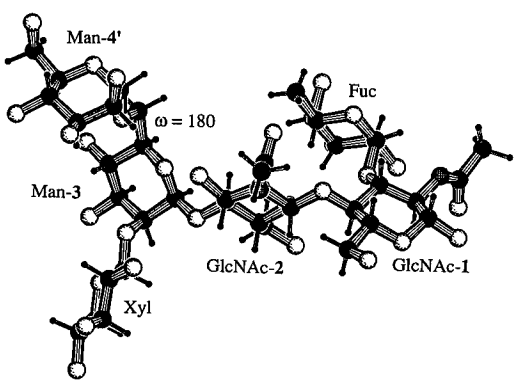

Fig. 8. *Molecular model of α-Man-(1→6)-[β-Xyl-(1→2)]-β-Man-(1→4)-β-GlcNAc-(1→4)-[α-Fuc-(1→3)]-β-GlcNAc for the* $P_{\omega=180}$ *rotamer*

been proposed, as indicated in Fig. 8 of [47]. The NMR data presented in this paper, however, show that for the closely related α-Man-(1→6)-[β-Xyl-(1→2)]-β-Man-(1→4)-β-GlcNAc-(1→4)-[α-Fuc-(1→3)]-β-GlcNAc-(1→N)-Asn∼ the $P_{\omega=180}$ rotamer is the dominating one. Molecular modelling, using the various calculated φ/ψ torsional angles and ω = 180 for the C-5 – C-6 linkage of β-Man, yielded a model as presented in Fig. 8.

This investigation was supported by the Netherlands Foundation for Chemical Research (SON) with financial aid from the Netherlands Organization for Scientific Research (NWO).

REFERENCES

1. Ishihara, H., Takahashi, N., Oguri, S. & Tejima, S. (1979) *J. Biol. Chem. 254*, 10715 – 10719.
2. Hase, S., Koyama, S., Daiyasu, H., Takemoto, H., Hara, S., Kobayashi, Y., Kyogoku, Y. & Ikenaka, T. (1986) *J. Biochem. (Tokyo) 100*, 1 – 10.
3. Takahashi, N., Hotta, T., Ishihara, H., Mori, M., Tejima, S., Bligny, R., Akazawa, T., Endo, S. & Arata, Y. (1986) *Biochemistry 25*, 388 – 395.
4. Van Kuik, J. A., Hoffmann, R. A., Mutsaers, J. H. G. M., Van Halbeek, H., Kamerling, J. P. & Vliegenthart, J. F. G. (1986) *Glycoconj. J. 3*, 27 – 34.
5. Sturm, A., Van Kuik, J. A., Vliegenthart, J. F. G. & Chrispeels, M. J. (1987) *J. Biol. Chem. 262*, 13392 – 13403.
6. Ashford, D., Dwek, R. A., Welply, J. K., Amatayakul, S., Homans, S. W., Lis, H., Taylor, G. N., Sharon, N. & Rademacher, T. W. (1987) *Eur. J. Biochem. 166*, 311 – 320.
7. Fournet, B., Leroy, Y., Wieruszeski, J.-M., Montreuil, J., Poretz, R. D. & Goldberg, R. (1987) *Eur. J. Biochem. 166*, 321 – 324.
8. D'Andrea, G., Bouwstra, J. B., Kamerling, J. P. & Vliegenthart, J. F. G. (1988) *Glycoconj. J. 5*, 151 – 157.
9. Kimura, Y., Hase, S., Kobayashi, Y., Kyogoku, Y., Ikenaka, T. & Funatsu, G. (1988) *J. Biochem. (Tokyo) 103*, 944 – 949.
10. Kimura, Y., Hase, S., Kobayashi, Y., Kyogoku, Y., Ikenaka, T. & Funatsu, G. (1988) *Biochim. Biophys. Acta 966*, 248 – 256.
11. Kimura, Y., Hase, S., Ikenaka, T. & Funatsu, G. (1988) *Biochim. Biophys. Acta 966*, 150 – 159.
12. Kimura, Y., Hase, S., Ikenaka, T. & Funatsu, G. (1988) *Biochim. Biophys. Acta 966*, 160 – 167.
13. Van Kuik, J. A., Van Halbeek, H., Kamerling, J. P. & Vliegenthart, J. F. G. (1985) *J. Biol. Chem. 260*, 13984 – 13988.

14. Van Kuik, J. A., Sijbesma, R. P., Kamerling, J. P., Vliegenthart, J. F. G. & Wood, E. J. (1986) *Eur. J. Biochem. 160*, 621–625.
15. Van Kuik, J. A., Sijbesma, R. P., Kamerling, J. P., Vliegenthart, J. F. G. & Wood, E. J. (1987) *Eur. J. Biochem. 169*, 399–411.
16. Bouwstra, J. B., Kerékgyártó, J., Kamerling, J. P. & Vliegenthart, J. F. G. (1989) *Carbohydr. Res. 186*, 39–49.
17. Kerékgyártó, J., Kamerling, J. P., Bouwstra, J. B., Vliegenthart, J. F. G. & Lipták, A. (1989) *Carbohydr. Res. 186*, 51–62.
18. Scocca, J. & Lee, Y. C. (1969) *J. Biol. Chem. 244*, 4852–4863.
19. Van Pelt, J., Damm, J. B. L., Kamerling, J. P. & Vliegenthart, J. F. G. (1987) *Carbohydr. Res. 169*, 43–51.
20. Kamerling, J. P. & Vliegenthart, J. F. G. (1982) *Cell Biol. Monogr. 10*, 95–125.
21. De Baaij, J. A., Janssen, F. W. & Voortman, G. (1986) *Sci. Tools 33*, 17–32.
22. Takahashi, N., Yasuda, Y., Kuzuya, M. & Murachi, T. J. (1969) *Biochemistry 66*, 659–667.
23. Aue, W. P., Bartholdi, E. & Ernst, R. R. (1976) *J. Chem. Phys. 64*, 2229–2246.
24. Rance, M., Sørensen, O. W., Bodenhausen, G., Wagner, G., Ernst, R. R. & Wüthrich, K. (1983) *Biochem. Biophys. Res. Commun. 117*, 479–485.
25. Marion, D. & Wüthrich, K. (1983) *Biochem. Biophys. Res. Commun. 113*, 967–974.
26. Braunschweiler, L. & Ernst, R. R. (1983) *J. Magn. Reson. 53*, 521–528.
27. Bax, A. & Davis, D. G. (1985) *J.Magn. Reson. 65*, 355–360.
28. Macura, S. & Ernst, R. R. (1980) *Mol. Phys. 41*, 95–117.
29. Kumar, A., Wagner, G., Ernst, R. R. & Wüthrich, K. (1981) *J. Am. Chem. Soc. 103*, 3654–3658.
30. Bax, A. (1983) *J. Magn. Reson. 53*, 517–520.
31. Rutar, V. (1984) *J. Magn. Reson. 58*, 306–310.
32. Wilde, J. A. & Bolton, P. H. (1984) *J. Magn. Reson. 59*, 343–346.
33. Breg, J., Romijn, D., Van Halbeek, H., Vliegenthart, J. F. G., Visser, R. A. & Haasnoot, C. A. G. (1988) *Carbohydr. Res. 174*, 23–36.
34. Sheldrick, B. & Akrigg, D. (1980) *Acta Crystallogr. B 36*, 1615–1621.
35. Bock, K. (1983) *Pure Appl. Chem. 55*, 605–622.
36. Kitaygorodsky, A. I. (1961) *Tetrahedron 14*, 230–236.
37. Venkatachalam, C. M. & Ramachandran, G. N. (1976) in *Conformation of biopolymers* (Ramachandran, G. N., ed.) vol. 1, p. 83, Academic Press, New York.
38. Thøgersen, H., Lemieux, R. U., Bock, K. & Meyer, B. (1982) *Can. J. Chem. 60*, 44–57.
39. Wu, G. D., Serianni, A. S. & Barker, R. (1983) *J. Org. Chem. 48*, 1750–1757.
40. Spek, A. L. (1982) *Computational crystallography* (Sayre, D., ed.) p. 528, Clarendon Press, Oxford.
41. Dijkstra, B. W., Vliegenthart, J. F. G., Strecker, G. & Montreuil, J. (1983) *Eur. J. Biochem. 130*, 111–115.
42. Hindsgaul, O., Norberg, T., Le Pendu, J. & Lemieux, R. U. (1982) *Carbohydr. Res. 109*, 109–142.
43. Berman, E. (1986) *Carbohydr. Res. 152*, 33–46.
44. Bock, K., Arnarp, J. & Lönngren, J. (1982) *Eur. J. Biochem. 129*, 171–178.
45. Homans, S. W., Dwek, R. A., Boyd, J., Mahmoudian, M., Richards, W. G. & Rademacher, T. W. (1986) *Biochemistry 25*, 6342–6350.
46. Brisson, J.-R. & Carver, J. P. (1983) *Biochemistry 22*, 3680–3686.
47. Homans, S. W., Dwek, R. A. & Rademacher, T. W. (1987) *Biochemistry 26*, 6571–6578.